

Article

Thermal Performance of Lightweight Steel Framed Facade Walls Using Thermal Break Strips and ETICS: A Parametric Study

Paulo Santos , Paulo Lopes  and David Abrantes

ISISE, Department of Civil Engineering, University of Coimbra, 3030-788 Coimbra, Portugal

* Correspondence: pfsantos@dec.uc.pt

Abstract: The thermal performance of lightweight steel framed (LSF) facade walls depends on many factors, such as the steel studs, the batt insulation, the external thermal insulation composite systems (ETICS), and the sheathing layers. Moreover, the high thermal conductivity of steel could negatively affect their thermal performance due to the consequent thermal bridge effect. Furthermore, in LSF walls, the batt insulation is usually bridged by the steel studs. Thus, some analytical calculation procedures defined in standards (e.g., ISO 6946) are not valid, further complicating their thermal performance quantification. In this research, a parametric study to evaluate the thermal performance of facade LSF walls is presented. Seven relevant parameters are assessed, most of them related to the use of thermal break strips (TBS) and ETICS. The 2D numerical models used to predict the conductive R -values were experimentally validated, and their precision was successfully verified. As earlier found in a previous research work for partition LSF walls, it is also more effective for facades to increase the TBS thickness rather than their width, with the R -value increments being slightly smaller for facade LSF walls. These features were more pronounced for double TBS and for the smaller stud spacing (400 mm). The major thermal performance improvements were found when increasing the ETICS insulation thickness and decreasing their thermal conductivity.

Keywords: thermal performance; lightweight steel framed; facade walls; thermal break strips; ETICS; parametric study



Citation: Santos, P.; Lopes, P.; Abrantes, D. Thermal Performance of Lightweight Steel Framed Facade Walls Using Thermal Break Strips and ETICS: A Parametric Study. *Energies* **2023**, *16*, 1699. <https://doi.org/10.3390/en16041699>

Academic Editor: Elena Lucchi

Received: 31 December 2022

Revised: 31 January 2023

Accepted: 5 February 2023

Published: 8 February 2023



Copyright: © 2023 by the authors. Licensee MDPI, Basel, Switzerland. This article is an open access article distributed under the terms and conditions of the Creative Commons Attribution (CC BY) license (<https://creativecommons.org/licenses/by/4.0/>).

1. Introduction

A thermal bridge, or cold bridge, can be defined as a localized zone of a building envelope which has a significantly higher heat transfer when compared to the adjacent areas [1]. Thermal bridges in buildings, regarding the way they are computed, can be categorized into three types: repeating thermal bridges (e.g., vertical steel studs equally spaced in a LSF wall), linear (nonrepeating) thermal bridges (e.g., along a projecting balcony, a wall-to-wall connection or a wall to floor edges), and point thermal bridges (e.g., the mechanical metallic fasteners to fix the insulation panels in ETICS).

Regarding the origin, there are usually two types of thermal bridges: geometric and construction thermal bridges. An example of a geometric thermal bridge is a wall-to-wall corner, given the higher outer surface area when compared to the inner one. Construction thermal bridges originate from a higher thermal conductivity of a specific localized material, such as a concrete column within a masonry ceramic brick wall.

Thermal bridges may lead to several negative consequences in buildings, such as increased heat transfer through the building envelope, localized colder zones in the inner sheathing surfaces, thermal discomfort of the occupants, moisture and condensation problems, mold growth, and decrease of materials' durability [1]. The ASIEPI research project [2] concluded that “the total impact of thermal bridges on the heating energy need is in general considerable and can be as high as 30%”. Moreover, Ge and Baba [3] simulated the dynamic effect of thermal bridges on the energy performance of reinforced concrete

residential building located in a hot climate and concluded that the presence of thermal bridges is able to increase the annual cooling load by 20%.

Given the high thermal conductivity of steel, the relevance of thermal bridges may be even higher if this issue is not adequately addressed at design stage and their mitigation strategies implemented during construction stage [4]. This is a very hot research topic, which has been addressed using several approaches, such as in situ or lab measurements [5–7], parametric studies [8–10], analytical evaluation [11], and numerical simulations [4,7].

Several thermal bridge mitigation strategies in LSF building elements have been developed and studied, including the use of steel profiles having indented flanges [10], the use of ETICS (external thermal insulation composite systems) [8,9,12,13], the placement of thermal break strips (TBS) along the steel studs flanges [5–7,9,10], and the application of steel studs with slotted webs [9,14].

There is no perfect thermal mitigation strategy since each one has its inherent drawbacks and advantages. The most frequent thermal bridge mitigation strategy is the use of ETICS. Being a continuous thermal insulation, the thermal performance improvement is more effective. Moreover, the building's net floor area is not reduced due to the additional ETICS thickness, since it is usually located outside the floor area [13]. On the other hand, since the very reduced insulation material's quantity used is placed only where it is needed more, i.e., along the steel stud flanges, the use of TBS is a highly cost-effective strategy to mitigate thermal bridges in LSF walls [5]. Nevertheless, the use of TBS may have a drawback due to the higher distance between the steel frame and the sheathing panels, equal to the TBS thickness, which will lead to a smaller mechanical resistance to lateral loading shear actions [15].

The steel stud flanges' indentation allows a reduction in the contact surface area between the sheathing panels and the steel, thereby reducing the heat transfer across the wall in the vicinity of the steel profile, without increasing the LSF wall thickness [10]. Moreover, an extra advantage is that the initial flange air gap can be filled with insulation material, similarly to a TBS, but without increasing the LSF wall thickness. Regarding the slotted steel studs strategy, the key disadvantage is related to the reduction in their load-bearing capacity [10].

In a previous study [16], the authors performed a parametric study about the use of thermal break strips (TBS) in load-bearing partition LSF walls, to mitigate the steel frame thermal bridges and improve their thermal performance. In this parametric study, five different parameters were assessed: (1) the steel stud distance, (2) the TBS position and number on the steel stud's flanges, (3) the TBS material's thermal conductivities, (4) the thicknesses, and (5) the width of TBS cross-section geometry. It was concluded that increasing the TBS width did not always lead to a thermal resistance improvement, and that increasing the TBS thickness is more effective than increasing their width, with this latter conclusion related to the volumetric expansibility of the mineral wool batt insulation.

A similar parametric study for load-bearing facade LSF walls was not found in the literature. Therefore, in the present research, a parametric study is performed for load-bearing facade LSF walls. In addition to the five abovementioned parameters, in the present parametric study, two more parameters are evaluated: (6) the thickness of the ETICS thermal insulation layer, and (7) their thermal conductivity. In this parametric study, bidimensional numerical models were used, which were experimentally validated, and their accuracy was successfully verified using three different additional strategies.

In this paper, after this brief introduction, Section 2 presents the materials and methods, including a description of the facade LSF wall used as reference, the evaluated parameters and their values, the characterization of the materials, and the numerical simulations. Next, the achieved results are presented and discussed in Section 3, starting by the reference facade LSF wall, followed by the results for a single TBS and for two TBSs, and finally the results about the relevance of ETICS insulation thickness and their thermal conductivity values. To finalize, the key conclusions of this study are presented in Section 4.

2. Materials and Methods

Here, the evaluated facade LSF walls are described, with emphasis on the reference one. Furthermore, the assessed parameters in this study are specified, including the geometry and dimensions of the TBS and ETICS, the steel stud spacing, and the materials used with their respective thermal properties. Next, the numerical simulations are described, including the domain discretization, the boundary conditions, the model validation, and accuracy verifications.

2.1. Reference Facade LSF Wall

Figure 1 displays the horizontal cross-section for the reference load-bearing facade LSF wall, used in this parametric study. The structure of the evaluated walls was made using vertical steel studs with a web of 90 mm, a flange of 43 mm, a lip return of 15 mm, and a sheet thickness of 1.5 mm. The wall cavity was fully filled with a mineral wool (MW) batt insulation, 90 mm thick. On both sides of the vertical studs, there was an oriented strand board (OSB) structural sheathing panel, 12 mm thick. Furthermore, in the inner surface there was an extra gypsum plasterboard (GPB), 12.5 mm thick, while, on the outer surface, there was an external thermal insulation composite system (ETICS), with expanded polystyrene (EPS) insulation, 50 mm thick, and an ETICS finishing layer, 5 mm thick.

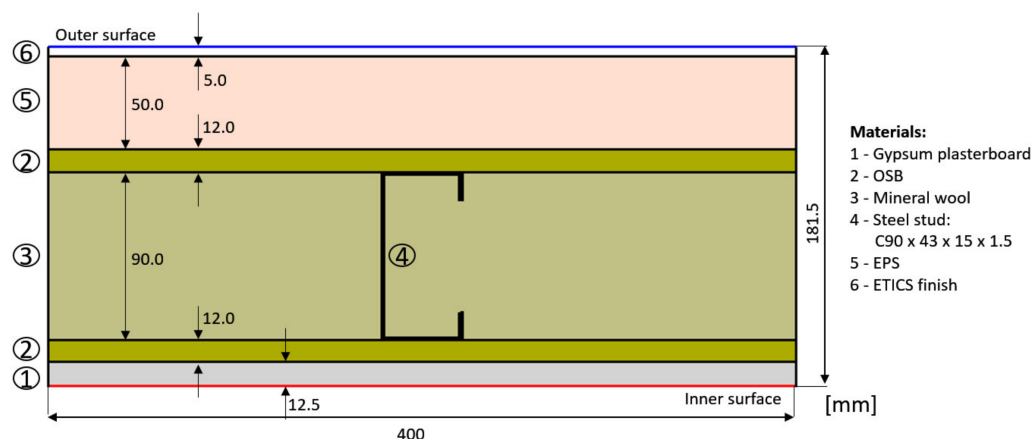


Figure 1. Horizontal cross-section of reference load-bearing facade LSF wall.

2.2. Evaluated Parameters

The parameters assessed in this parametric study, as well as the values to be used for each one, are listed in Table 1 and schematically illustrated in Figure 2. These parameters were (1) the spacing of the steel studs, (2) the dimensions (thickness and width), thermal conductivity, and number of the TBSs, and (3) the thickness and thermal conductivity of the ETICS insulation material. Note that, as illustrated in Figure 2, the addition of a TBS (single or double) increased the total LSF wall thickness and, given the high MW expansion capacity, it was assumed always a fully filled air cavity with this batt insulation.

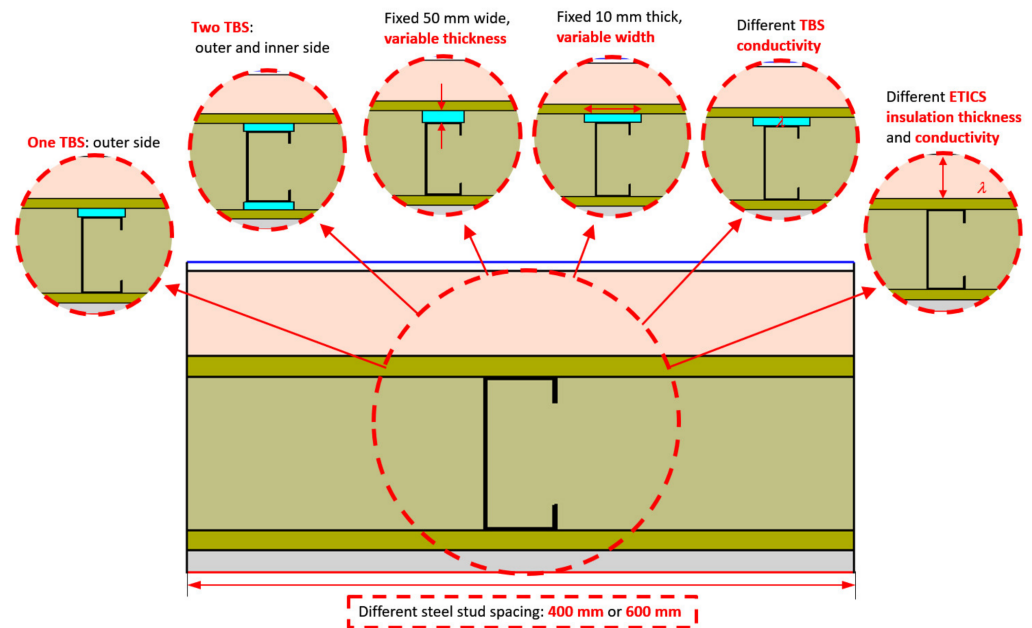
Table 1. Parameters of the facade LSF walls to be evaluated and assigned values.

Parameter	Values
Steel stud spacing [mm]	400 *, 600
Thermal Break Strips:	
-Thickness [mm]	5, 7.5, 10 *, 12.5, 15
-Width [mm]	30, 40, 50 *, 60, 70
-Conductivity [mW/(m·K)]	7.5, 15, 30 *, 60, 120
-Number	Zero *, one ² , two ³

Table 1. Cont.

Parameter	Values
ETICS ¹ :	
-Insulation thickness [mm]	30, 40, 50 *, 60, 70
-Insulation conductivity [mW/(m·K)]	7.5, 15, 30, 36 * ⁴ , 60, 120

* Reference values are in bold. ¹ ETICS—External thermal insulation composite system; ² one—outer flange; ³ two—both inner and outer flanges; ⁴ thermal conductivity value of the reference ETICS insulation material (EPS—expanded polystyrene).

**Figure 2.** Evaluated parameters of the facade LSF walls.

2.3. Material Characterization

Table 2 displays the materials used in the LSF walls, including the thickness, t , and the thermal conductivity, λ . Note that the TBSs were previously characterized in Table 1, regarding their evaluated dimensions (thickness and width) and assessed thermal conductivities.

Table 2. Thickness (t) and thermal conductivity (λ) of the materials used in the reference facade LSF wall.

Material	t [mm]	λ [W/(m·K)]	Ref.
Gypsum plaster board (GPB)	12.5	0.175	[17]
Oriented strand board (OSB)	12.0	0.100	[18]
Mineral wool (MW)	90.0	0.035	[19]
Steel studs (C90 × 43 × 15 × 1.5)	90.0	50.000	[20]
ETICS ² insulation (EPS ¹)	50.0	0.036	[21]
ETICS ² finish	5.0	0.450	[22]

¹ EPS—expanded polystyrene; ² ETICS—external thermal insulation composite system.

2.4. Numerical Simulations

To perform the numerical simulations of the evaluated facade LSF walls, the software THERM (version 7.6.1) [23] was used. In this subsection, some relevant details related to the implemented THERM finite element method (FEM) models are explained, including the discretization of the domain, the employed boundary conditions, the model validation, and accuracy verifications.

2.4.1. Domain Discretization

The materials' thermal properties and dimensions were previously presented in Tables 1 and 2. It was only needed to model a representative part of the LSF walls' cross-section, as displayed previously in Figure 1. This strategy allowed decreasing the calculation effort and time. Moreover, the numerical computation error of the implemented FEM models was capped at 2%.

2.4.2. Boundary Conditions

To perform the numerical simulations, two sets of boundary conditions were set: (1) the environment air temperatures, and (2) the surface thermal resistances. For this parametric study, the external environment temperature was set as 0 °C, as for the usual outdoor winter season temperature in mild climates. Moreover, the interior environment temperature was set to 20 °C, as for the usual indoor comfort temperature in the winter season. Note that the computed thermal resistance (or R -value) does not depend on the adopted temperatures indoor or outdoor environment temperatures, as prescribed by standard ISO 6946 [24]. This same standard recommends some default values for the surface thermal resistances. In this study, these standardized values were adopted, specifically 0.04 m²·K/W for external surface thermal resistance (R_{se}) and 0.13 m²·K/W for internal surface thermal resistance (R_{si}).

2.4.3. Model Accuracy Verifications and Validation

Three precision verifications and one validation procedure were realized to ensure the reliability of the bidimensional THERM software [23] models.

Regarding the models' accuracy verifications, the references were as follows: (1) the Annex C, ISO 10211 standard [25] 2D test cases; (2) the analytical calculation procedures defined in standard ISO 6946 [24]; (3) the 3D FEM simulation results provided by ANSYS software [26].

Regarding the model validation, the results were compared with some experimental measurements, under controlled laboratory conditions, as depicted in the next subsection.

(1) ISO 10211 Test Cases Verification

For this verification, the two bidimensional test cases depicted in Annex C of standard ISO 10211 [25] were modeled, and the results obtained were within the bounds permitted, ensuring the precision of the THERM algorithm and the models. For sake of brevity and to avoid repetitions, the results are not displayed here. However, they can be accessed in previous studies from the authors [13,27,28].

(2) ISO 6946 Analytical Calculus Verification

Since standard ISO 6946 [24] provides some analytical calculation procedures for walls having homogeneous layers, a simplified LSF wall THERM model was built, assuming no steel frame. For this accuracy verification, the THERM model was very similar to the one previously illustrated in Figure 1, for the reference facade LSF wall, but having no steel stud. Moreover, the material's properties were also the same (see Table 2), as well as the boundary conditions (see Section 2.4.2).

The computed thermal transmittances for the numerical and analytical approaches are displayed in Table 3. Both obtained U -values were the same, highlighting the excellent accuracy and reliability of the THERM models.

Table 3. Thermal transmittance calculated for the simplified reference facade LSF wall assuming homogeneous layers (without steel stud).

LSF Wall Type	U-Value [W/(m ² ·K)]	
	Numerical (THERM)	Analytical (ISO 6946)
Facade	0.225	0.225

(3) 3D FEM Verification

In this precision verification, a comparison between the 2D model results, obtained using the THERM software [23], and the 3D model results, computed using the ANSYS software [26], was performed. Two different facade LSF walls were assessed: (1) the reference LSF wall without any TBS (previously illustrated in Figure 1); (2) a similar LSF wall containing an outer TBS, having a thermal conductivity equal to 30 mW/(m·K), a width equal to 50 mm, and 10 mm thickness. All other thicknesses and thermal conductivities were early displayed in Table 2, and the implemented boundary conditions were the same as described in Section 2.4.2.

The computed conductive *R*-values and the isothermal colour distribution are displayed in Figure 3a for the reference facade LSF wall (without TBS) and in Figure 3b for a similar wall having a TBS along the outer steel stud flange. The greatest difference between 2D and 3D models occurred for the reference LSF facade (+0.5%), while, for the other LSF wall configuration having a TBS, the difference was almost negligible (−0.001 m²·K/W, 0.0%), again demonstrating the exceptional accuracy of the THERM models used in this parametric study.

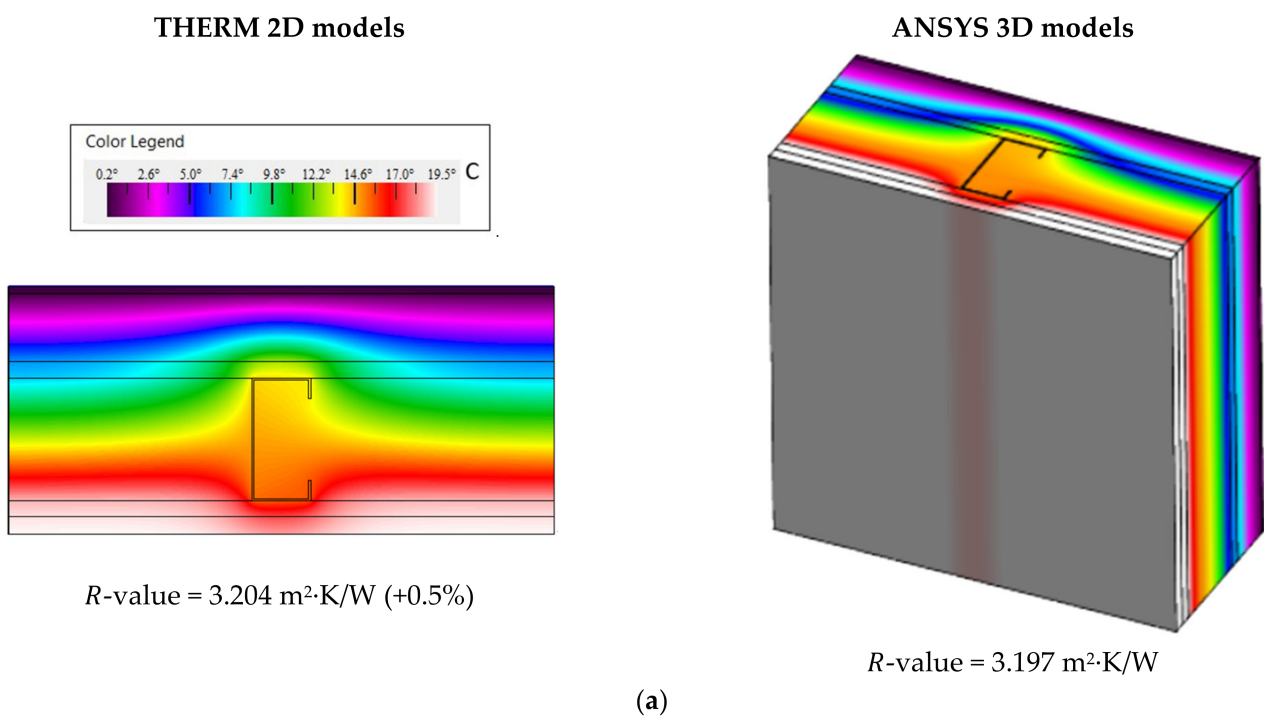


Figure 3. Cont.

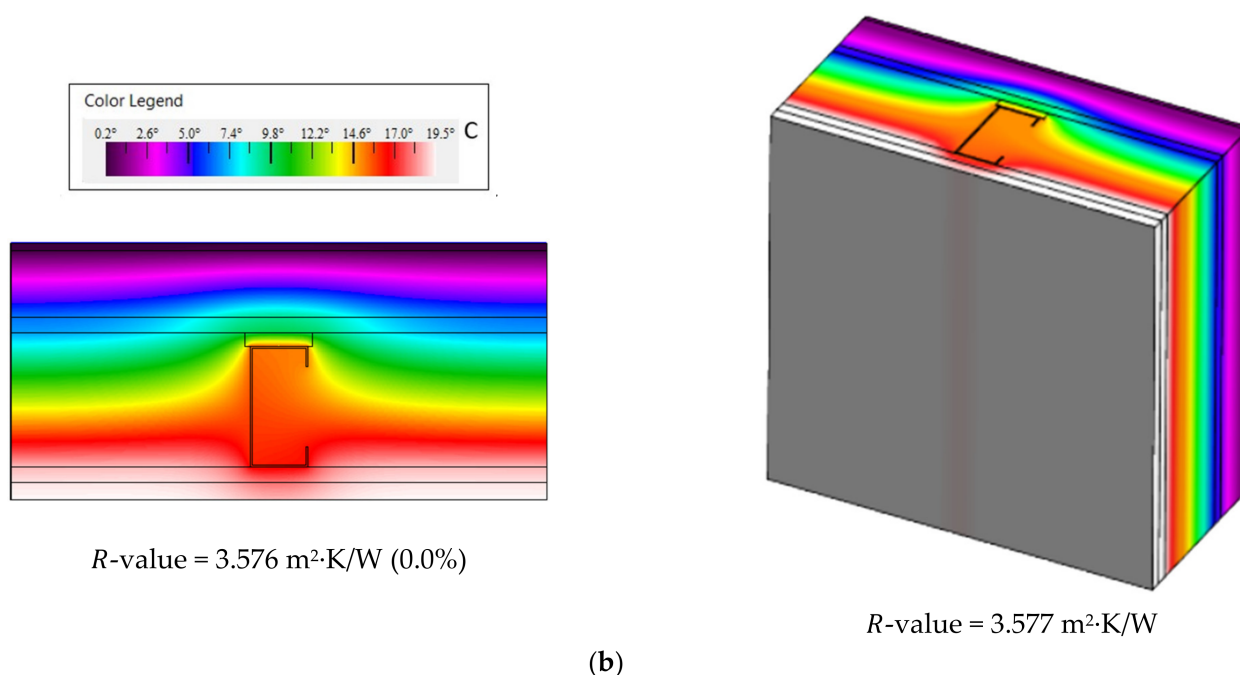


Figure 3. Accuracy verification of the LSF facade wall model: temperature distribution and R -values: (a) reference LSF facade; (b) LSF facade with an outer thermal break strip.

(4) Lab Measurement Validation

The THERM model for the reference facade LSF wall, in addition to the three previous explained accuracy verifications, was also validated against lab measurements, under controlled conditions. These laboratory measurements were performed using the same test procedures and setup as those described in previous research from the same authors [16], for the thermal performance evaluation of load-bearing partition LSF walls. Therefore, for the sake of conciseness and to avoid unnecessary repetitions, these test procedures and lab setup are not explained here again.

Nevertheless, the achieved results for the reference facade LSF wall are displayed in Table 4, which lists the measured conductive thermal resistances for the three height sensor locations and the equivalent average conductive R -value (3.200 m²·K/W). Note that the conductive thermal resistance computed by the THERM model is also shown in this table (3.204 m²·K/W). This very reduced difference between the measured and the predicted thermal resistances (only +0.1%) allowed ensuring the precision of these THERM models, but also permitted their validation.

Table 4. Reference facade LSF wall conductive R -values, for both experimental and numerical methods.

Test	Sensors Location	R -Value [m ² ·K/W]
1	Top	3.247
2	Middle	3.121
3	Bottom	3.232
Measurement Average		3.200
Computed in THERM		3.204
Percentage Deviation		+0.1%

3. Results and Discussion

In this section, the computed results are displayed and analyzed. First, the R -values for the reference facade LSF wall are presented. Then, the thermal performance of this LSF facade wall is evaluated when using a single TBS, placed in the outer steel stud flange. Next, the use of two TBS is assessed. Lastly, the influence of the ETICS insulation thermal conductivity and thickness, when there is no TBS, is also analyzed.

3.1. Reference Facade LSF Wall

The reference surface-to-surface thermal resistance for the facade LSF wall with commercial $C90 \times 43 \times 15 \times 1.5$ steel studs, placed 400 mm apart (Figure 1), is $3.204 \text{ m}^2 \cdot \text{K}/\text{W}$ (Figure 3a). For the 600 mm steel stud spacing, the R -value is improved to $3.499 \text{ m}^2 \cdot \text{K}/\text{W}$ (+9%). This thermal performance improvement of the LSF facade wall was expected, due to the decreased amount of steel, originating from the increased steel studs' spacing.

3.2. One Thermal Break Strip

3.2.1. The Influence of TBS Thickness and Thermal Conductivity

The surface-to-surface thermal resistances obtained for the facade LSF walls, having one TBS with variable thickness and 50 mm width, for two different steel stud spacings ((a) 400 mm; (b) 600 mm), are displayed in Figure 4. The current charts show the same trend as those described in the previous study [16], but it can be noted that, on these facade LSF walls (having ETICS), the TBS performance improvement was smaller than in the previous partition LSF walls. This could be explained by the reduced relevance of the steel studs' thermal bridges due to the ETICS insulation continuous layer.

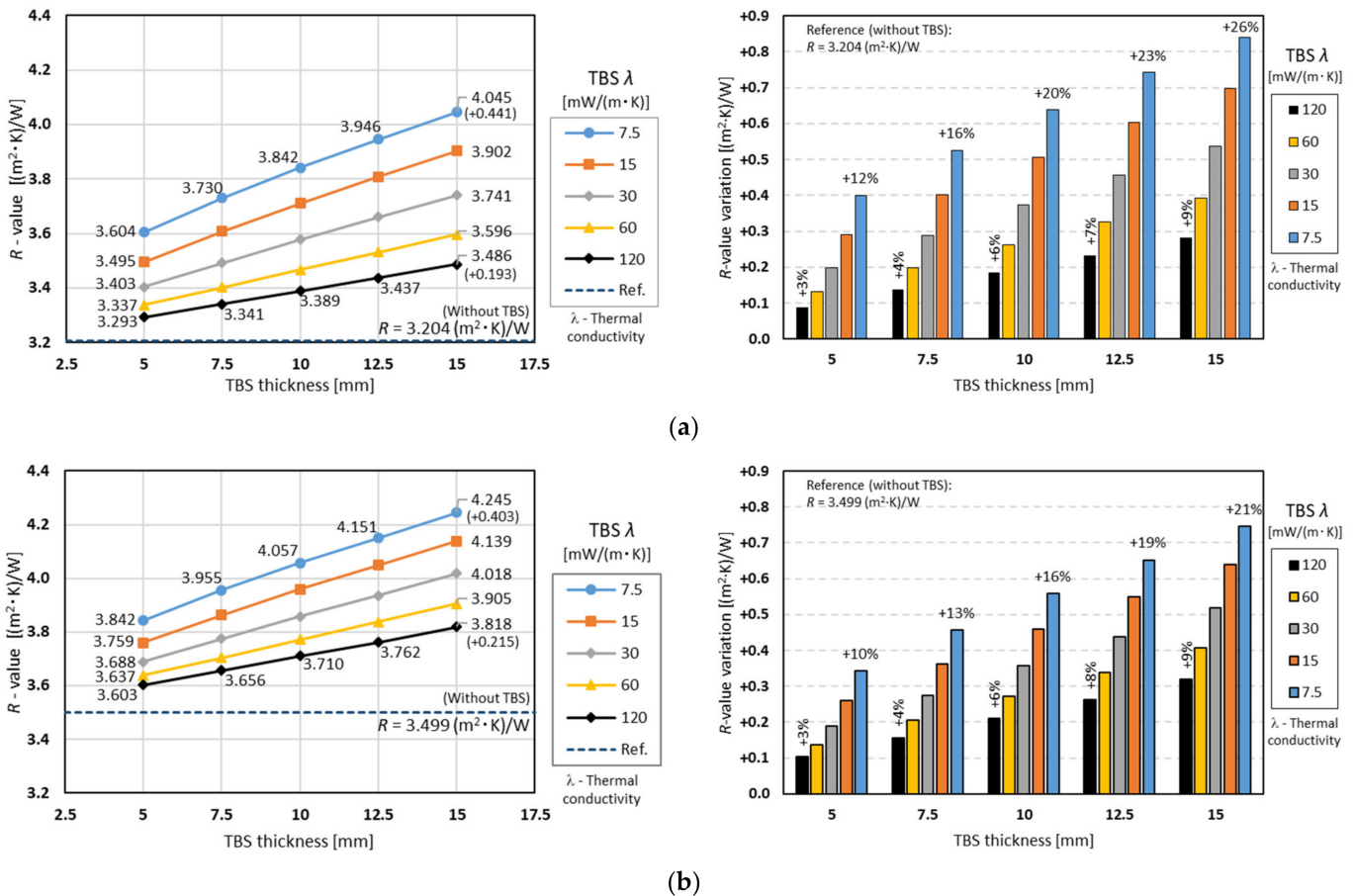


Figure 4. Surface-to-surface thermal resistances for facade LSF walls, having one thermal break strip with variable thickness and 50 mm wide, for two different steel stud spacings: (a) 400 mm; (b) 600 mm.

Nevertheless, with respect to the R -values presented in Figure 4a for the higher thermal conductivity (120 mW/m·K; black line), even the thinner TBS (5 mm) allowed increasing the thermal performance from 3.204 m²·K/W (reference value) to 3.293 m²·K/W. Moreover, when there was an increase in the TBS thickness up to 15 mm, the thermal resistance also had a nearly linear variation increase, up to 3.486 m²·K/W. In terms of percentages (see right plot), these R -value increments range from +3% to +9%.

Looking now to the other evaluated smaller TBS thermal conductivities, the slope of the corresponding R -values lines also increased with the decrease in TBS conductivity. This trend was predictable, and the major R -values were achieved for the smaller TBS thermal conductivity (7.5 mW/m·K, blue line), varying from 3.604 m²·K/W (5 mm thick) up to 4.045 m²·K/W (15 mm thick). As displayed in the right graph of Figure 4a, this thermal resistance variation, in relation to the reference facade LSF wall, increased from +12% (5 mm thick) to +26% (15 mm thick).

Two analogous plots are displayed in Figure 4b for 600 mm steel stud spacing, instead of 400 mm spacing. As predicted, all computed R -values were bigger than the preceding ones, including the new reference one (3.449 m²·K/W). Moreover, for the same TBS thickness, the R -value increase originating from the TBS thermal conductivity decrease was now smaller relatively to the former studs' spacing (400 mm), illustrated in Figure 4a.

Additionally, in both plots (400 mm and 600 mm steel studs' spacing), increasing the TBS thickness always provided an improved thermal performance, regardless of the conductivity. This is due to the assumed mineral wool batt insulation's volumetric expansibility, fulfilling the increased wall cavity, whereby this wall thickness increment is equal to the TBS thickness.

3.2.2. The Influence of TBS Width and Thermal Conductivity

Figure 5a exhibits the surface-to-surface R -values obtained for the facade LSF walls having one TBS with variable width and constant thickness (10 mm), when the steel studs are spaced 400 mm. With respect to the R -values for the thermal conductivity equal to 120 mW/m·K (higher evaluated value; black line), even the smaller assessed TBS width (30 mm) enabled an R -value increase from 3.204 m²·K/W (reference value) to 3.447 m²·K/W. However, when the TBS width increased to 70 mm, the R -value decreased to 3.361 m²·K/W, i.e., a negative variation equal to -0.086 m²·K/W. Looking now to the thermal conductivity of 30 mW/m·K (gray line), the R -value variation was very reduced (+0.018 m²·K/W) when increasing the width of the TBS (3.564 to 3.582 m²·K/W). Observing now the smaller evaluated TBS conductivity R -values (blue line), there was a major increment relative to the reference facade LSF wall (3.204 to 3.675 m²·K/W), as well as when increasing the TBS width from 30 to 70 mm (+0.264 m²·K/W). In terms of percentages (see blue vertical bars in the right plot of Figure 5a), this R -value increment ranged from +15% to +23%.

The computed R -values for a larger steel studs' spacing (600 mm) are displayed in Figure 5b. Comparing this new plot with the previous one (Figure 5a), the major differences are the higher predicted R -values and the reduced thermal performance variations due to the use of TBS. In fact, the R -value reduction for the higher TBS conductivity (120 mW/m·K; black line) became -0.068 m²·K/W, instead of the previous decrease of -0.086 m²·K/W. Observing the smaller TBS conductivity (7.5 mW/m·K; blue line), the thermal resistance increment, due to the TBS width increase, became (Figure 5b, 600 mm) only +0.197 m²·K/W, when the previous value (Figure 5a, 400 mm) was +0.264 m²·K/W.

Comparing Figures 4 and 5, it can be observed that a TBS having 10 mm thickness and 30 mm width (Figure 5) presented higher R -values in comparison to a TBS having 5 mm thickness and 50 mm width (Figure 4), regardless of the steel studs' spacing and the TBS conductivity. However, increasing the TBS thickness (Figure 4) was always more gainful (higher R -values increment) in comparison to a TBS width increase (Figure 5). Moreover, for the higher evaluated TBS conductivity values (60 and 120 mW/m·K), it was not adequate to increase the TBS width, since there was a consequent reduction in the facade LSF wall thermal performance (Figure 5). Thus, similarly to a previous study for partition

LSF walls [16], it can also be concluded for facade LSF walls that it is more effective to increase the thickness than the width of the TBS. However, in facade LSF walls, the thermal performance improvement due to the use of TBS was smaller, since the steel studs' thermal bridges were less relevant, due to the existence of a facade ETICS continuous insulation.

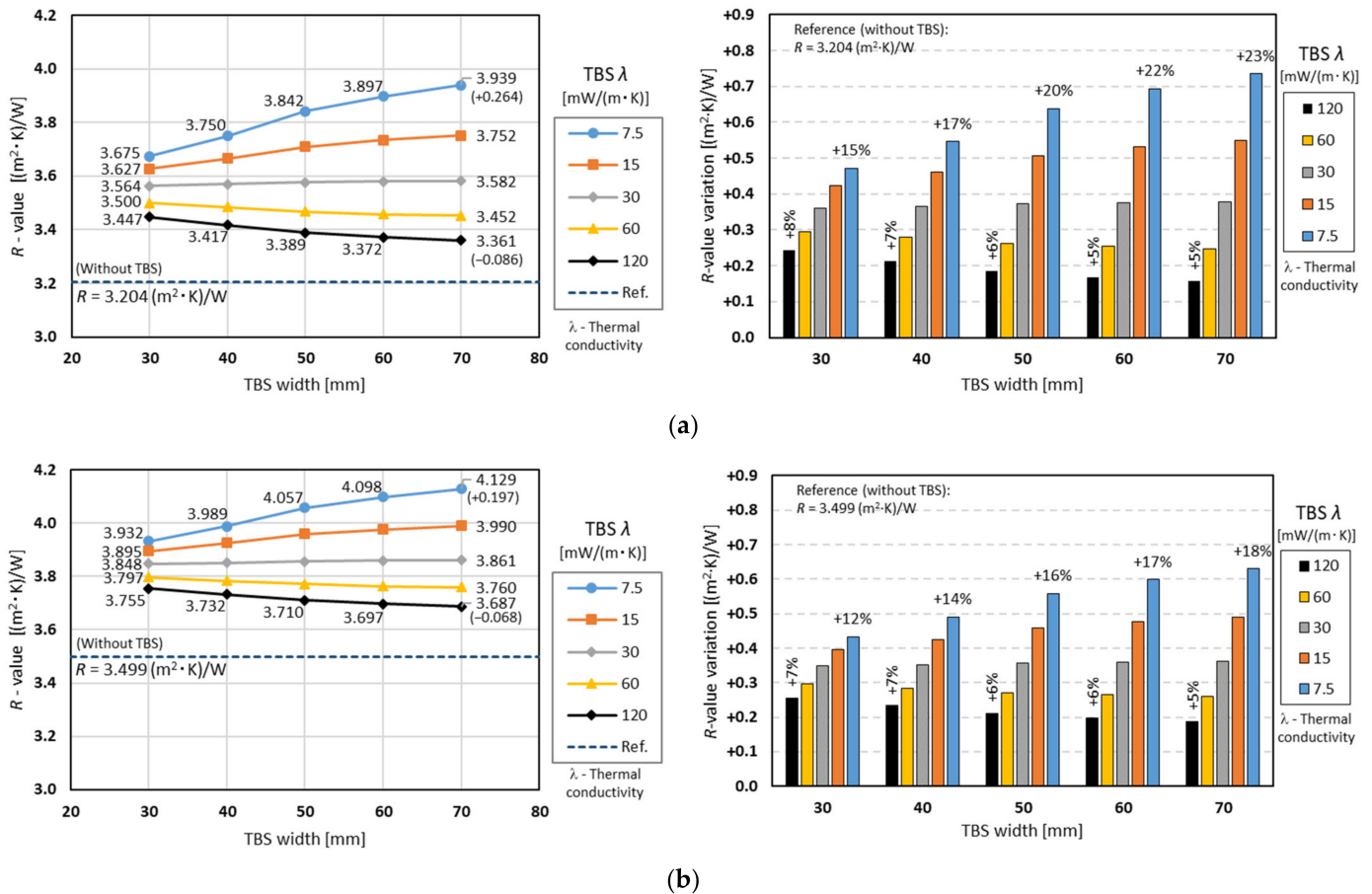


Figure 5. Surface-to-surface thermal resistances for facade LSF walls, having one thermal break strip with variable width and 10 mm thick, for two different steel stud spacings: (a) 400 mm; (b) 600 mm.

3.3. Two Thermal Break Strips

This subsection presents and discusses the computed R -values for facade LSF walls when using two TBS, instead of only one outer TBS.

3.3.1. The Influence of TBS Thickness and Thermal Conductivity

Figure 6a is similar to Figure 4a, but with the facade LSF walls having two TBSs instead of a single outer TBS. These new charts exhibit very similar features to the previous ones but with higher R -values. This was expected given the use of two TBS and their consequent thermal performance improvement. As mentioned before, this thermal performance enhancement was due not only to the use of the TBS itself, but also to the consequent increase in the wall air cavity and batt insulation thickness, which was equal to the thickness summation of both TBSs (10 + 10 mm).

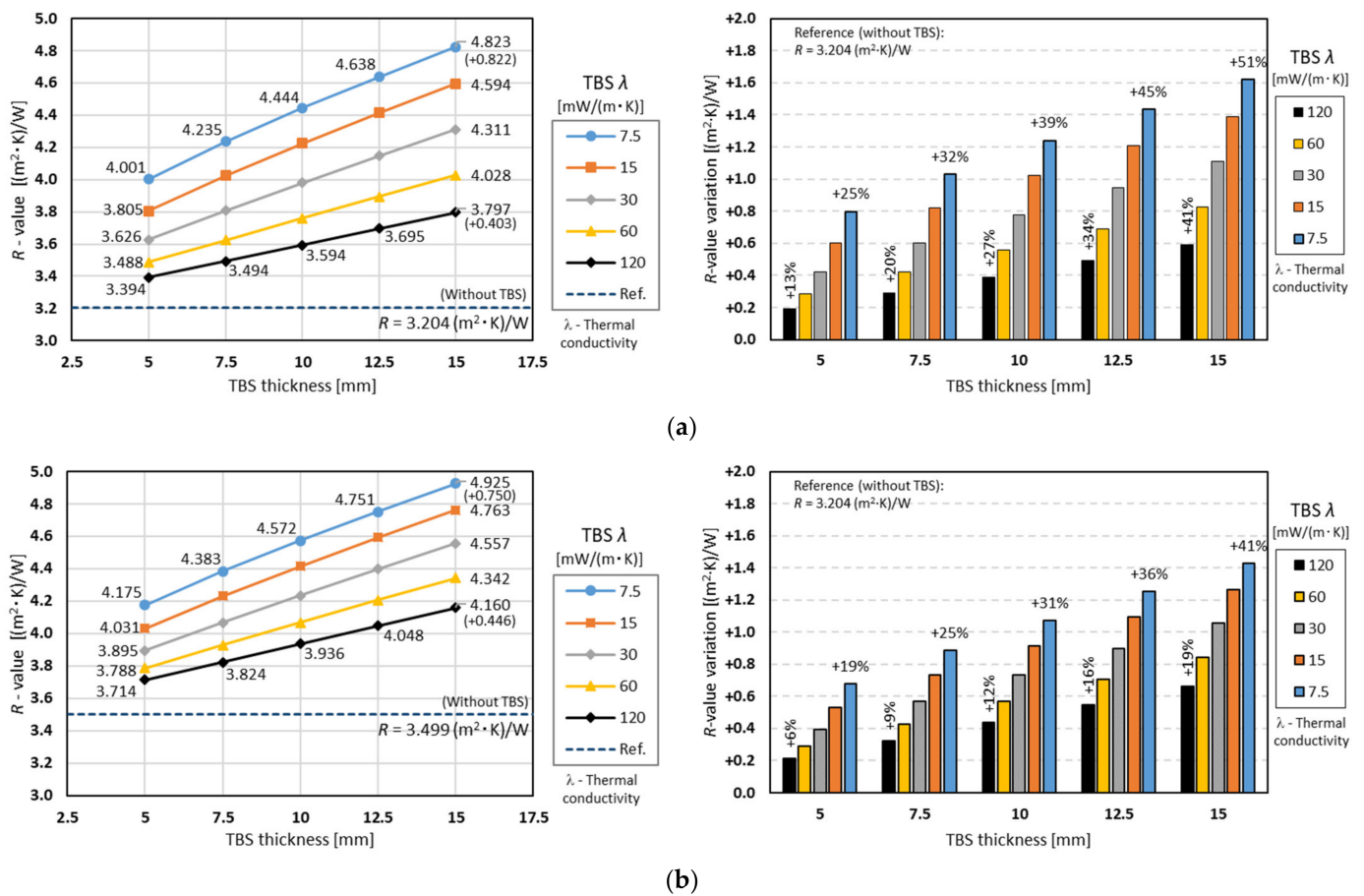


Figure 6. Surface-to-surface thermal resistances for facade LSF walls, having two thermal break strips with variable thickness and 50 mm wide, for two different steel stud spacings: (a) 400 mm; (b) 600 mm.

Other interesting findings could be obtained when comparing the case where the total thickness of TBSs was the same, but the number was different (one and two). For example, according to the blue line ($\lambda = 7.5$ mW/m·K) in the left graph of Figure 4a, the R -value was 3.842 [m²·K)/W] when the thickness was 10 mm (one TBS), while, according to the left graph of Figure 6a, the R -value was 4.001 [(m²·K)/W] when the thickness of each TBS was 5 mm (the total thickness of two TBSs was 10 mm). This appears to indicate that it is more effective to split the TBSs (higher thermal resistance) instead of using a single one with the same total thickness.

The computed results for a 600 mm steel stud spacing is displayed in Figure 6b, exhibiting a similar trend to that for a 400 mm spacing (Figure 6a); however, all obtained R -values were higher than the previous ones, as anticipated given the smaller steel amount per wall square meter and consequent minor steel-related thermal bridge effect. Moreover, in Figure 6b, for the same TBS thickness, the thermal performance improvement due to the TBS conductivity decrease was now quite smaller when compared to the 400 mm steel stud spacing (Figure 6a). Additionally, the R -value increment due to the TBS thickness increase was reduced for smaller TBS conductivities (e.g., 7.5 mW/m·K; blue line), +0.750 instead of +0.822 m²·K/W, and slightly increased for higher thermal conductivity values (e.g., 120 mW/m·K; black line), +0.446 instead of +0.403 m²·K/W.

3.3.2. The Influence of TBS Width and Thermal Conductivity

Figure 7a is analogous to Figure 5a. However, instead of a single outer TBS, the facade LSF walls have two TBSs, i.e., one in the outer stud flange and another TBS in the inner flange. The trends exhibited in these two plots are identical, but with an improved thermal performance, i.e., increased R -values. In addition to this enhanced thermal performance,

the relevance of increasing the TBS width was higher for the same TBS conductivity, which was expected since two TBSs were used (Figure 7a) instead of one (Figure 5a). In fact, for the smaller TBS conductivity (7.5 mW/m·K; blue line), the R -value increment was +0.430 $m^2 \cdot K/W$, instead of only +0.264 $m^2 \cdot K/W$. Moreover, for the higher evaluated TBS conductivity (120 mW/m·K; black line), the thermal resistance decrease was $-0.169 m^2 \cdot K/W$, instead of $-0.086 m^2 \cdot K/W$.

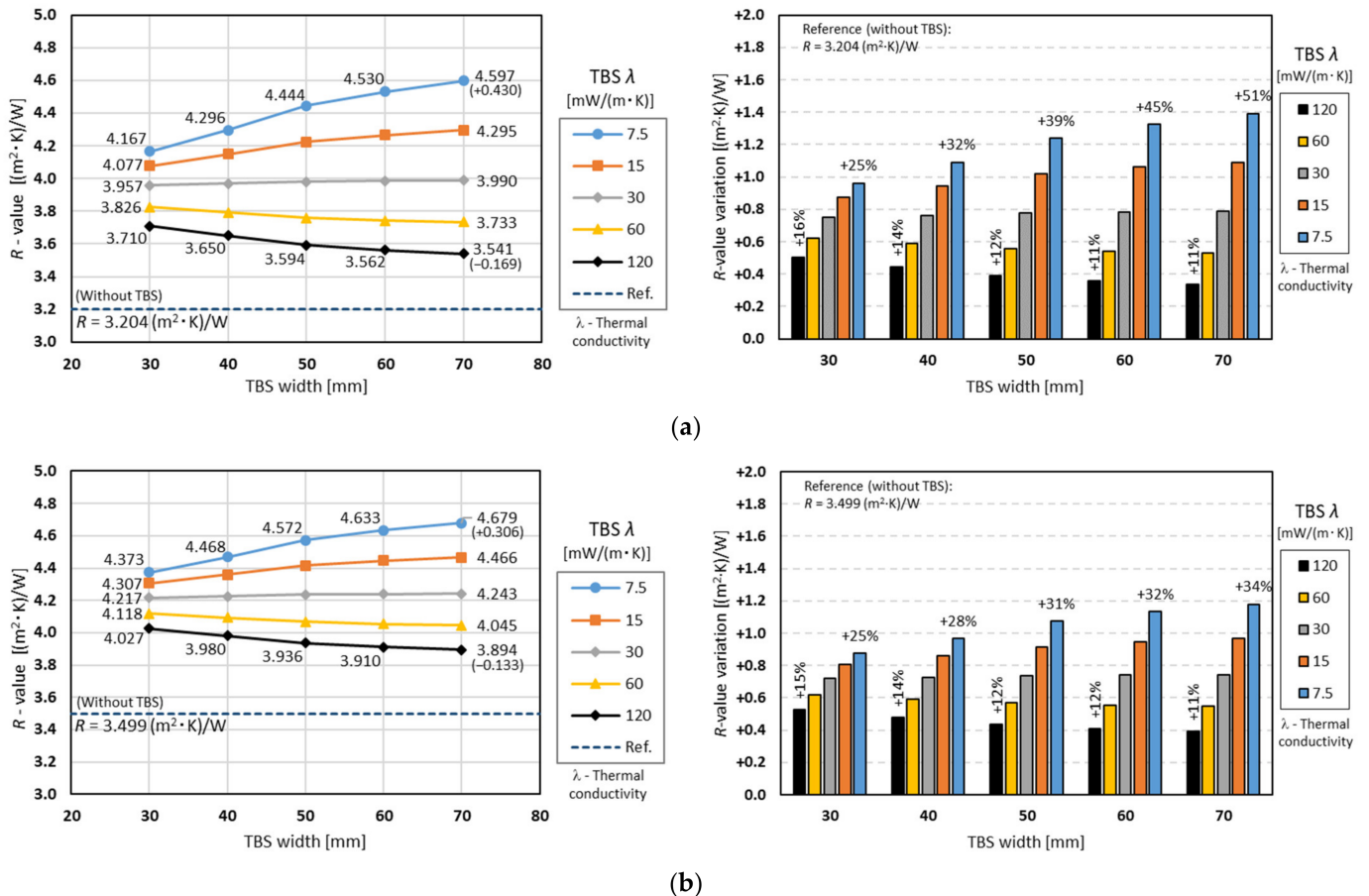


Figure 7. Surface-to-surface thermal resistances for facade LSF walls, having two thermal break strips with variable width and 10 mm thick, for two different steel stud spacings: (a) 400 mm; (b) 600 mm.

The predicted R -values for an increased steel stud spacing (600 mm, instead of 400 mm) are plotted in Figure 7b. As seen before for a single TBS (Figure 5), this chart had an identical tendency, but now all predicted R -values were bigger when compared to the previous ones (Figure 7a, 400 mm stud spacing), including the reference one (3.499 $m^2 \cdot K/W$), as mentioned before. Furthermore, the relevance of the TBS conductivity for the same TBS width, and the relevance of the TBS width for the same thermal conductivity were now smaller, when compared to the previous steel stud spacing (400 mm).

3.4. ETICS Insulation Thickness and Thermal Conductivity

In addition to the use of one (see Section 3.2) or two TBSs (see Section 3.3), this research assessed the relevance of changing the ETICS insulation thickness and thermal conductivity to improve the thermal performance of facade LSF walls. Figure 8a illustrates the computed surface-to-surface R -values, for facade LSF walls having ETICS insulation thickness changing from 30 to 70 mm and thermal conductivity values ranging between 7.5 and 120 mW/m·K, with a steel stud spacing equal to 400 mm, without TBS.

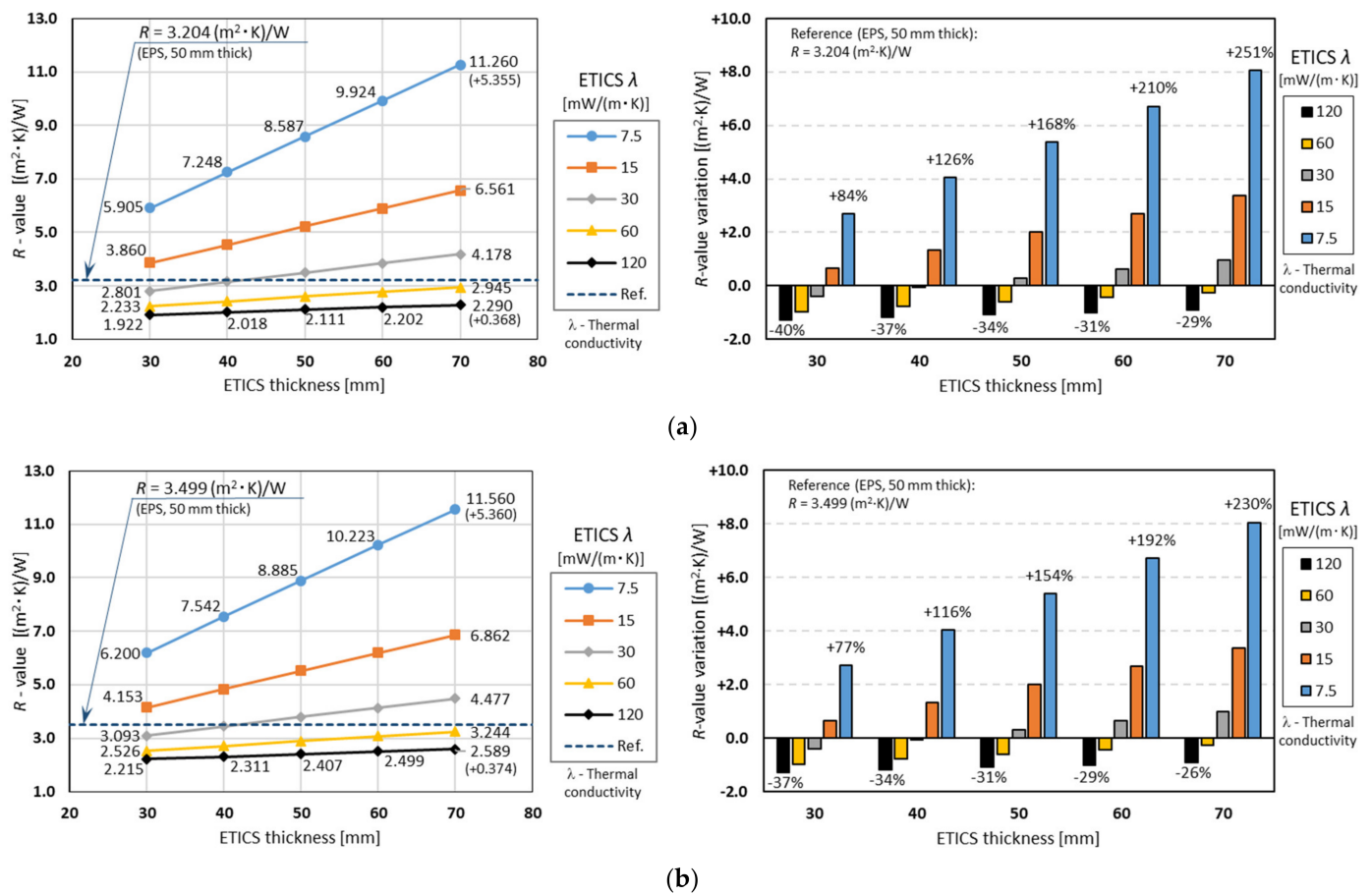


Figure 8. Surface-to-surface thermal resistances for facade LSF walls, without thermal break strips, having a variable ETICS insulation thickness and thermal conductivity, for two different steel stud spacings: (a) 400 mm; (b) 600 mm.

Compared to previous plots (one and two TBS), several main differences arise, such as (1) the ETICS insulation thermal conductivity lines for higher values (30, 60 and 120 mW/m·K) having smaller thermal resistances in relation to the reference facade LSF wall R-value (3.204 m²·K/W), (2) the R-values variation range now being much larger, ranging (70 mm ETICS thickness) from 2.290 m²·K/W up to 11.260 m²·K/W, for the 120 and 7.5 mW/m·K insulation thermal conductivities, respectively, and (3) the thermal resistance increment with the ETICS insulation thickness increase now also being larger, mainly for the smaller thermal conductivities (e.g., +5.360 m²·K/W for 7.5 mW/m·K, blue line).

Figure 8b shows the same parameters variation, but for LSF walls having a 600 mm steel stud spacing. In comparison to the previous steel stud spacing (400 mm) chart (Figure 8a), the main features are as follows: (1) as expected, due to the minor steel content per LSF wall area, all R-values were now increased; (2) however, the R-value increment due to ETICS insulation thickness increase, for each thermal conductivity value, was very similar (as expected, since this insulation layer was continuous). Note that, in terms of percentages, the R-value increment seemed larger for the 400 mm stud spacing (Figure 8a, left), but this was mainly due to a smaller reference R-value (3.204 instead of 3.499 m²·K/W).

As illustrated in Figure 8b, insulation materials with smaller thermal conductivities, 7.5 and 15 mW/m·K, exhibited higher thermal performance, with maximum R-values (for 70 mm thickness and 600 mm steel stud spacing) of 11.560 and 6.862 (m²·K)/W, respectively. Not surprisingly, for insulation materials with higher thermal conductivities, 60 and 120 mW/m·K, the R-value of the reference wall (having 50 mm of EPS thermal insulation, 36 mW/m·K) was not reached. Moreover, even for a smaller thermal conductivity

(30 mW/m·K; gray line), when the thickness was reduced (30 and 40 mm), the achieved R -values were also smaller than the reference one (3.499 m² K/W).

4. Conclusions

In this article, a parametric study related to the thermal performance of load-bearing facade LSF walls was completed. This research is a continuation of a previous parametric study for partition LSF walls from the same authors [16]. In the present study, seven parameters were assessed: (1) the steel stud distance; (2) the TBS position and number along the steel stud's flanges; (3) the thermal conductivity of the TBS material; (4) the TBS thickness; (5) the TBS width; (6) the thickness of the ETICS thermal insulation layer; (7) the thermal conductivity.

The reliability of the obtained results was ensured by the experimental validation of the bidimensional THERM [23] models, which were used to simulate the thermal performance of the assessed facade LSF walls. Additionally, their accuracy was also successfully verified using three different approaches.

The main outcomes of this research are summarized as follows:

- The increase in the steel stud spacing from 400 mm to 600 mm allowed an R -value thermal performance improvement of +0.295 m²·K/W, which is very similar to the result achieved previously for partition LSF walls: +0.292 m²·K/W [16].
- Similarly to what was concluded before for load-bearing partition LSF walls [16], for load-bearing facade LSF walls, it is still more effective to increase the TBS thickness rather than their width.
- Nevertheless, the R -value increments are slightly smaller for facade LSF walls, due to the existence of an ETICS continuous thermal insulation layer, which decreases the steel studs' thermal bridges relevance, as expected.
- The previous features are valid for one or two TBSs placed along the vertical steel studs, but are more pronounced for the double TBS.
- The major thermal performance improvements were found when increasing the ETICS insulation thickness (from 30 to 70 mm) and decreasing their thermal conductivity (to 7.5 mW/m·K), for which it was found a relevant R -value increase of +5.360 m²·K/W, for a 400 mm steel stud spacing.
- In fact, the abovementioned thermal performance improvement was significantly higher (around 6.5 times) than the most relevant one achieved when using two TBSs, having 15 mm thickness (increased from 5 mm), 50 mm width, and 7.5 mW/m·K thermal conductivity, which was only +0.822 m²·K/W, for the reference steel stud spacing (400 mm).

Regarding the foremost limitations of this study, one can mention that all other steel profiles of the facade LSF wall were neglected, considering only the vertical load-bearing steel studs. Secondly, several batt insulation materials are available on the market, but only one was modeled (mineral wool). With respect to the first constraint, it can be mentioned that the modeled vertical load-bearing steel studs were the most frequent and relevant ones in facade LSF walls. Moreover, some other steel frame profiles (e.g., bottom and top wall trackers) are usually considered within the slab to contribute to the wall linear thermal bridge effect, which was outside of the scope of this study. Concerning the second restriction, mineral wool is perhaps the most used batt insulation material today. Moreover, it was supposed that this fibrous insulation material has enough expandability to fill the cavity of the facade LSF wall.

Through this work, it was possible to better comprehend, compare, and quantify the thermal performance improvement due to the use of TBS and ETICS in load-bearing facade LSF walls. Such a systematic parametric study did not previously exist in the literature. At the design stage, this knowledge could be advantageous for engineers and designers when there is a necessity to specify the TBS material, width, thickness, and number, as well as the ETICS insulation material and thickness.

Author Contributions: Conceptualization, P.S.; Methodology, P.S., P.L. and D.A.; Validation, P.S. and P.L.; Formal analysis, P.L. and D.A.; Investigation, P.S., P.L. and D.A.; Resources, P.S.; Writing—original draft, P.L. and D.A.; Writing—review & editing, P.S.; Visualization, P.S. and D.A.; Supervision, P.S.; Project administration, P.S.; Funding acquisition, P.S. All authors have read and agreed to the published version of the manuscript.

Funding: This research was funded by FEDER funds through the Competitiveness Operational Program—COMPETE, and by national funds through FCT, Foundation for Science and Technology, within the scope of the project POCI-01-0145-FEDER-032061.

Cofinanciado por: POCI-01-0145-FEDER-032061



Acknowledgments: The authors also want to thank the following companies: Pertecno, Gyptec Ibéria, Volcalis, Sotinco, Kronospan, Hulkseflux, Hilti, and Metabo.

Conflicts of Interest: The authors declare no conflict of interest.

References

- Santos, P.; da Silva, L.S.; Ungureanu, V. *Energy Efficiency of Light-Weight Steel-Framed Buildings*, 1st ed.; Technical Committee 14-Sustainability & Eco-Efficiency of Steel Construction; European Convention for Constructional Steelwork (ECCS): Brussels, Belgium, 2012; ISBN 978-92-9147-105-8.
- Erhorn-Kluttig, H.; Erhorn, H. *Impact of Thermal Bridges on the Energy Performance of Buildings*; European Commission: Brussels, Belgium, 2009; pp. 1–8.
- Ge, H.; Baba, F. Dynamic effect of thermal bridges on the energy performance of a low-rise residential building. *Energy Build.* **2015**, *105*, 106–118.
- Gomes, A.P.; de Souza, H.A.; Tribess, A. Impact of thermal bridging on the performance of buildings using Light Steel Framing in Brazil. *Appl. Therm. Eng.* **2013**, *52*, 84–89. [[CrossRef](#)]
- Santos, P.; Mateus, D. Experimental assessment of thermal break strips performance in load-bearing and non-load-bearing LSF walls. *J. Build. Eng.* **2020**, *32*, 101693.
- Santos, P.; Abrantes, D.; Lopes, P.; Mateus, D. Experimental and Numerical Performance Evaluation of Bio-Based and Recycled Thermal Break Strips in LSF Partition Walls. *Buildings* **2022**, *12*, 1237. [[CrossRef](#)]
- Santos, P.; Mateus, D.; Ferrandez, D.; Verdu, A. Numerical Simulation and Experimental Validation of Thermal Break Strips' Improvement in Facade LSF Walls. *Energies* **2022**, *15*, 8169.
- Kapoor, D.R.; Peterman, K.D. Quantification and prediction of the thermal performance of cold-formed steel wall assemblies. *Structures* **2021**, *30*, 305–315.
- Martins, C.; Santos, P.; Simoesdasilva, L. Lightweight steel-framed thermal bridges mitigation strategies: A parametric study. *J. Build. Phys.* **2016**, *39*, 342–372. [[CrossRef](#)]
- Santos, P.; Poologanathan, K. The Importance of Stud Flanges Size and Shape on the Thermal Performance of Lightweight Steel Framed Walls. *Sustainability* **2021**, *13*, 3970. [[CrossRef](#)]
- Santos, P.; Lemes, G.; Mateus, D. Analytical Methods to Estimate the Thermal Transmittance of LSF Walls: Calculation Procedures Review and Accuracy Comparison. *Energies* **2020**, *13*, 840. [[CrossRef](#)]
- Kosny, J.; Christian, J.E. Thermal evaluation of several configurations of insulation and structural materials for some metal stud walls. *Energy Build.* **1995**, *22*, 157–163.
- Santos, P.; Gonçalves, M.; Martins, C.; Soares, N.; Costa, J.J. Thermal transmittance of lightweight steel framed walls: Experimental versus numerical and analytical approaches. *J. Build. Eng.* **2019**, *25*, 100776. [[CrossRef](#)]
- Lupan, L.M.; Manea, D.L.; Moga, L.M. Improving Thermal Performance of the Wall Panels Using Slotted Steel Stud Framing. *Procedia Technol.* **2016**, *22*, 351–357.
- Henriques, J.; Rosa, N.; Gervasio, H.; Santos, P.; da Silva, L.S. Structural performance of light steel framing panels using screw connections subjected to lateral loading. *Thin-Walled Struct.* **2017**, *121*, 67–88.
- Santos, P.; Lopes, P.; Abrantes, D. Thermal Performance of Load-Bearing, Lightweight, Steel-Framed Partition Walls Using Thermal Break Strips: A Parametric Study. *Energies* **2022**, *15*, 9271. [[CrossRef](#)]
- Gyptec Ibérica. Technical Sheet: Standard Gypsum Plasterboard. 2022. Available online: https://www.gyptec.eu/documentos/Ficha_Tecnica_Gyptec_A.pdf (accessed on 10 February 2022).
- Kronospan. *Technical Sheet: Kronobuild Materials*; KRONOSPAN GmbH: Steinheim-Sandebeck, Germany, 2022.
- Volcalis. Technical Sheet: Alpha Mineral Wool. 2022. Available online: https://www.volcalis.pt/categoria_file_docs/fichatecnica_volcalis_alpharollo-386.pdf (accessed on 10 February 2022).
- Santos, C.; Matias, L. *ITE50-Coefficientes de Transmissão Térmica de Elementos da Envolvente dos Edifícios (in Portuguese)*; LNEC-Laboratório Nacional de Engenharia Civil: Lisboa, Portugal, 2006.
- LNEC. *Documento de Homologação: Tincoterm EPS-Sistema Compósito de Isolamento Térmico pelo Exterior*; LNEC: Maia, Portugal, 2015.

22. WEBERTHERM UNO. Technical Sheet: Weber Saint-Gobain ETICS Finish Mortar (in Portuguese). 2018. Available online: www.pt.weber/files/pt/2019-04/FichaTecnica_weberthermuno.pdf (accessed on 14 March 2019).
23. THERM. Software version 7.6.1. Lawrence Berkeley National Laboratory, United States Department of Energy. 2017. Available online: <https://windows.lbl.gov/software/therm> (accessed on 14 February 2019).
24. *ISO 6946*; Building Components and Building Elements—Thermal Resistance and Thermal Transmittance—Calculation Methods. International Organization for Standardization: Geneva, Switzerland, 2017.
25. *ISO 10211*; Thermal Bridges in Building Construction—Heat Flows and Surface Temperatures—Detailed Calculations Ponts Thermiques Dans les Bâtiments—Flux Thermiques et Températures Superficielles—Calculs Détaillés COPYRIGHT PROTECTED DOCUMENT. International Organization for Standardization: Geneva, Switzerland, 2017.
26. ANSYS Workbench, Software version 19.1; ANSYS, Inc.: Canonsburg, PA, USA, 2018. Available online: www.ansys.com/products/ (accessed on 8 June 2020).
27. Roque, E.; Santos, P. The Effectiveness of Thermal Insulation in Lightweight Steel-Framed Walls with Respect to Its Position. *Buildings* **2017**, *7*, 13.
28. Santos, P.; Lemes, G.; Mateus, D. Thermal Transmittance of Internal Partition and External Facade LSF Walls: A Parametric Study. *Energies* **2019**, *12*, 2671. [[CrossRef](#)]

Disclaimer/Publisher’s Note: The statements, opinions and data contained in all publications are solely those of the individual author(s) and contributor(s) and not of MDPI and/or the editor(s). MDPI and/or the editor(s) disclaim responsibility for any injury to people or property resulting from any ideas, methods, instructions or products referred to in the content.